

University of Nebraska - Lincoln

DigitalCommons@University of Nebraska - Lincoln

Anthony F. Starace Publications

Research Papers in Physics and Astronomy

January 1998

Novel Doubly Excited States Produced in Negative Ion Photodetachment

Anthony F. Starace

University of Nebraska-Lincoln, astarace1@unl.edu

Follow this and additional works at: <https://digitalcommons.unl.edu/physicsstarace>



Part of the [Physics Commons](#)

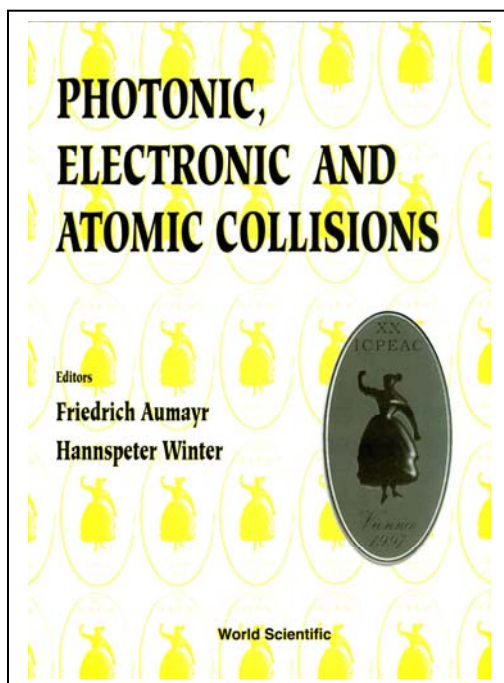
Starace, Anthony F., "Novel Doubly Excited States Produced in Negative Ion Photodetachment" (1998). *Anthony F. Starace Publications*. 120.

<https://digitalcommons.unl.edu/physicsstarace/120>

This Article is brought to you for free and open access by the Research Papers in Physics and Astronomy at DigitalCommons@University of Nebraska - Lincoln. It has been accepted for inclusion in Anthony F. Starace Publications by an authorized administrator of DigitalCommons@University of Nebraska - Lincoln.

Published in *Photonic, Electronic and Atomic Collisions: Invited Papers of the Twentieth International Conference on The Physics of Electronic and Atomic Collisions*, Vienna, Austria, July 23–29, 1997. Edited by Friedrich Aumayr and Hannspeter Winter. Singapore, New Jersey, London, Hong Kong: World Scientific, 1998).

Copyright © World Scientific Publishing Co. Pte. Ltd.
Used by permission.



NOVEL DOUBLY EXCITED STATES PRODUCED IN NEGATIVE ION PHOTODETACHMENT

ANTHONY F. STARACE^a

*Department of Physics and Astronomy, The University of Nebraska,
Lincoln, NE 68588-0111, U.S.A.*

Eigenchannel R -matrix calculations for photodetachment partial cross sections of H^- , Li^- , Na^- , and Al^- provide results that are dominated by high doubly-excited states and that are in excellent agreement with available measurements. Propensity rules for doubly-excited states developed for H^- apply also for heavier targets. However, states not observed in H^- may be observed in the heavier target spectra owing to the non-Coulomb core. Finally the signature of particular doubly excited states changes drastically from one partial cross section to another.

1 Introduction

Photodetachment of negative ions near excited atomic thresholds provides an opportunity to study correlated, three-body Coulomb states unencumbered by Rydberg series. Only with the advent of powerful computer workstations have theorists been able to carry out numerical calculations for such high, doubly excited states with spectroscopic accuracy. At the same time, improvements in laser technology have enabled a number of experimental groups to obtain detailed experimental data in the vicinity of excited state thresholds. Thus theory and experiment have recently been progressing together, with each reinforcing and challenging the other.

Experimental measurements of doubly-excited state atomic spectra have long served as stimuli for novel theoretical descriptions of correlated electronic states. Indeed, the first measurements of He doubly-excited state spectra below the $He^+(n=2)$ threshold¹ led theorists to abandon the independent-particle model in order to properly describe the observed experimental intensities.^{2,3} Recent experimental measurements of doubly-excited state spectra for H^- ⁴ and for He^5 in the vicinity of much higher detachment or ionization thresholds (i.e., below the $H(n)$ or $He^+(n)$ thresholds, where $n > 2$) have been interpreted by theorists as reflecting propensity rules for populating particular channels of '+'-type doubly-excited states.^{6,7,8,9,10,11} These experimental and theoretical advances have focused on the He and H^- two-electron systems, as these represent the prototypes for the study of correlated electronic states.

^aWork carried out in collaboration with Chien-Nan Liu and Cheng Pan at the University of Nebraska-Lincoln and with Chris H. Greene at the University of Colorado-Boulder.

A motivation for our studies of negative alkali and other negative ions was to discover how the structures which appear in H^- are modified by the non-Coulomb cores of these heavier systems. In particular, we were interested in finding out whether doubly excited states which are absent in the H^- spectrum do indeed become visible in the spectra of heavier negative ions. Our calculations employ the eigenchannel R -matrix method.^{12,13,14,15} In order to successfully obtain converged results, the close-coupling equations without exchange are solved outside the R -matrix sphere. In this progress report we illustrate some of our findings obtained from calculations for H^- ,¹⁶ Li^- ,^{16,17,18} Na^- ,¹⁸ and Al^- .¹⁹

2 H^- and Li^- Photodetachment Below the $H(n=5)$ and $Li(n=5)$ Thresholds

In order to compare Li^- photodetachment with H^- photodetachment, we must take account of the non-degeneracy of the atomic Li excitation thresholds. We therefore add together the $Li(n\ell)$ partial cross sections and compare with the $H(n)$ partial cross section. Fig. 1 shows the partial cross sections for exciting the $n=4$ states of the neutral atoms plotted against energy relative to the appropriate double ionization threshold.¹⁶ On a coarse energy scale the two spectra are very similar, particularly at higher energies. The prominent series of window resonances (whose first members are labelled *a*) are strong features of both spectra. The weak features (whose first members are labelled *b*) are, however, different in the two spectra. These differences stem from the exact degeneracy of the H atom levels compared to the lack of degeneracy in the Li atom.

To make connection with predicted propensity rules and to identify the

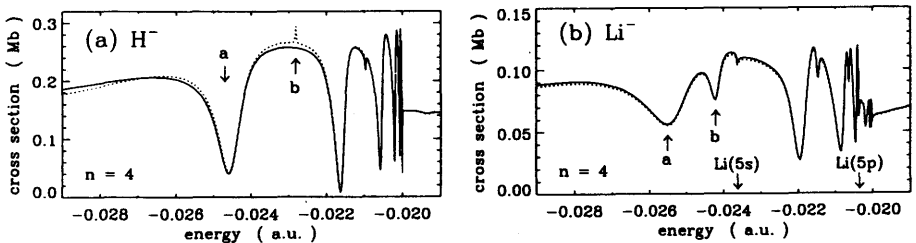


Figure 1: (a) Photodetachment cross sections for the process $H^- + \gamma \rightarrow H(n=4) + e^-$. (b) Photodetachment cross sections for the process $Li^- + \gamma \rightarrow Li^-(n=4) + e^-$. The abscissae show the final state energy relative to the double ionization threshold. Full curves, present dipole velocity results; broken curves present dipole length results. Labels *a* and *b* denote doubly-excited resonances having “+” (*i.e.*, an antinode) and “-” (*i.e.*, a node) respectively in their probability distribution along the Wannier ridge line, $r_1 = r_2$. (From Pan *et al.*¹⁶)

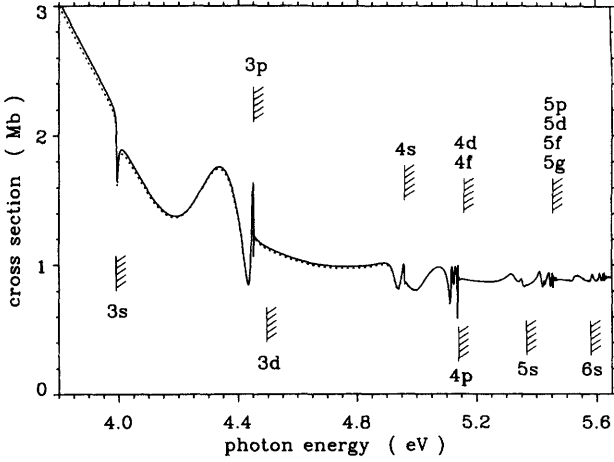


Figure 2: Calculated total photodetachment cross section for Li^- for photon energies from 3.8 eV to 5.65 eV. Full (dotted) curves give dipole velocity (length) results. The $\text{Li}(nl)$ thresholds in this energy region are indicated. (From Pan *al.*¹⁷)

features in the calculated cross sections, special R -matrix calculations were carried out with an interaction volume V of radius $r_0 = 120$ a.u. All basis functions were set to zero on the boundary of V . Thus only the discrete structures were calculated, in order to see which ones appeared at the energies corresponding to the features seen in the cross sections shown in Fig. 1. Resonances were found at the energies indicated by a and b in Fig. 1 in each system. When the probability distributions for these two-electron resonances are plotted,¹⁶ one finds that the a resonances have a strong antinode along the Wannier ridge (at $r_1 = r_2$) whereas the b resonances have a node. In H^- this node for the b resonance is nearly exact, whereas in Li^- it is more approximate. For this reason the b resonance is predicted to produce a distinct window resonance feature in the Li^- photodetachment spectrum, whereas it is predicted to be only evident as an extremely sharp, narrow feature in H^- .

3 Comparison of Li^- Photodetachment Cross Sections with Experiment

Our results¹⁷ for the Li^- total photodetachment cross section are shown in Fig. 2 with all excitation thresholds indicated. Above the 3p threshold features in the cross section are difficult to discern. As shown below, however, the partial cross sections are dominated by doubly-excited state resonance structures.

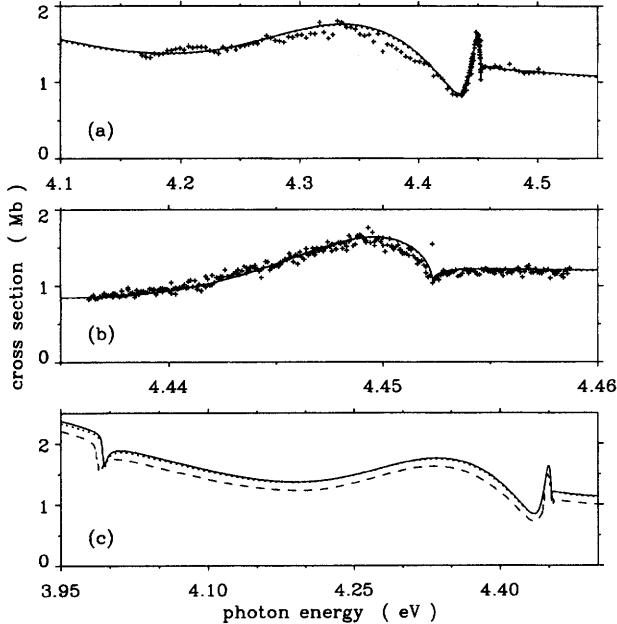


Figure 3: Comparison of calculated total photodetachment cross sections in dipole velocity (solid curve) and dipole length (dotted curve) approximation of Pan *et al.*¹⁷ with experimental results (+) of Berzinsh *et al.*²⁰ Relative experimental results are normalized to our theoretical velocity curve at $\hbar\omega = 4.45\text{eV}$. (a) $4.1 \leq \hbar\omega \leq 4.55$ eV. (b) Detail of the vicinity of the Li(3p) threshold. (c) Comparison with theoretical results (dashed curve) of Lindroth.^{20,21} (From Ref. 17.)

The energy region between the Li(3s) and Li(3p) thresholds was investigated in detail by Pan *et al.*¹⁷ because of the possibility of comparisons with both experimental²⁰ and other theoretical^{20,21} data. The comparisons are shown in Fig. 3. Both on the broad energy scale shown in Fig. 3(a) and on the fine energy scale shown in Fig. 3(b) (near the 3p threshold), our calculated total detachment cross section shows a very accurate prediction of experimentally observed features. Fig. 3(c) compares our total cross section results with those of Lindroth^{20,21}; there is excellent qualitative agreement, although our results lie $\approx 5\% - 10\%$ higher in this energy region.

Doubly excited states in the vicinity of the Li(3s) and Li(3p) thresholds hold the key to interpreting the features observed in Fig. 3 in the Li⁻ photodetachment cross section (such as the broad minimum and subsequent maximum near 4.2 eV and 4.35 eV respectively as well as the sharper minimum and subsequent maximum just below the 3p threshold). Prior theoretical studies

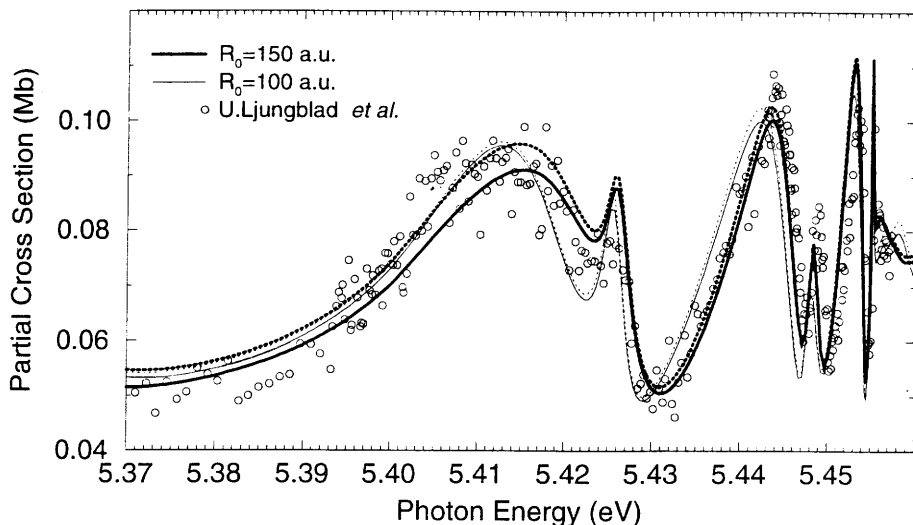


Figure 4: Comparison of theoretical calculations of Liu and Starace¹⁸ employing an R -matrix sphere of $R_o = 150$ a.u. with both results of Pan *et al.*¹⁷ for $R_o = 100$ a.u. and with experimental results of Ljungblad *et al.*²³ for the process $\text{Li}^- + \gamma \rightarrow \text{Li}(3s) + e^-$ in the energy region below the $\text{Li}(5p)$ threshold at about 5.455 eV.

of Li^- doubly-excited state resonances below the $3p$ threshold predict only a single $^1P^o$ resonance located near the $\text{Li}(3p)$ threshold (cf. Ref. 17 for references and a detailed discussion). In a non-standard calculation,¹⁷ we found two resonances below the $\text{Li}(3p)$ threshold at 4.22 eV and 4.44 eV. The lowest resonance is very well-localized, whereas the higher one, lying just below the $\text{Li}(3p)$ threshold, is not. Furthermore, removing the effects of these two resonances in our calculated cross sections gives “background” cross sections that are smooth and structureless, providing strong evidence that these doubly-excited states control the observed cross sections. We find that the lowest resonance is the “ $3s3p$ ” resonance first calculated by Lin.²² It has a distinct antinode along the $r_1 = r_2$ Wannier ridge and dominates the behavior of the Li^- photodetachment cross section below the $\text{Li}(3p)$ threshold. Because the second resonance we obtained is so diffuse and close in energy to the $\text{Li}(3p)$ threshold, it is not certain that it is truly bound (because inclusion of the $3s$ orbital in our non-standard calculation introduces coupling with continuum channels). Nevertheless, the second resonance we obtain is the major influence on the detachment cross section near the $\text{Li}(3p)$ threshold.

We have calculated all partial cross sections for the process $\text{Li}^- + \gamma \rightarrow \text{Li}(n\ell) + e^-$ up to the $6s$ level. Recently Ljungblad *et al.*²³ measured the

Li(3s) partial cross section below the Li(4p) and Li(5p) thresholds. Below the Li(4p) threshold, experiment is in excellent agreement with our predictions,¹⁷ but below the Li(5p) threshold discrepancies were found. As the discrepancies appeared only near the highest excitation thresholds, we carried out new calculations¹⁸ employing a much larger R -matrix sphere radius. The results are shown in Fig. 4. Agreement between theory and experiment is now greatly improved, particularly above the minimum at about 5.43 eV. Theory still, however, predicts a sharp resonance feature at about 5.425 eV that is only hinted at by the experimental data. We have found that there are three resonances which describe the major features seen in Fig. 4; in particular, the sharp feature at 5.425 eV has significant contributions from 5pnd and 5dnf configurations.¹⁸

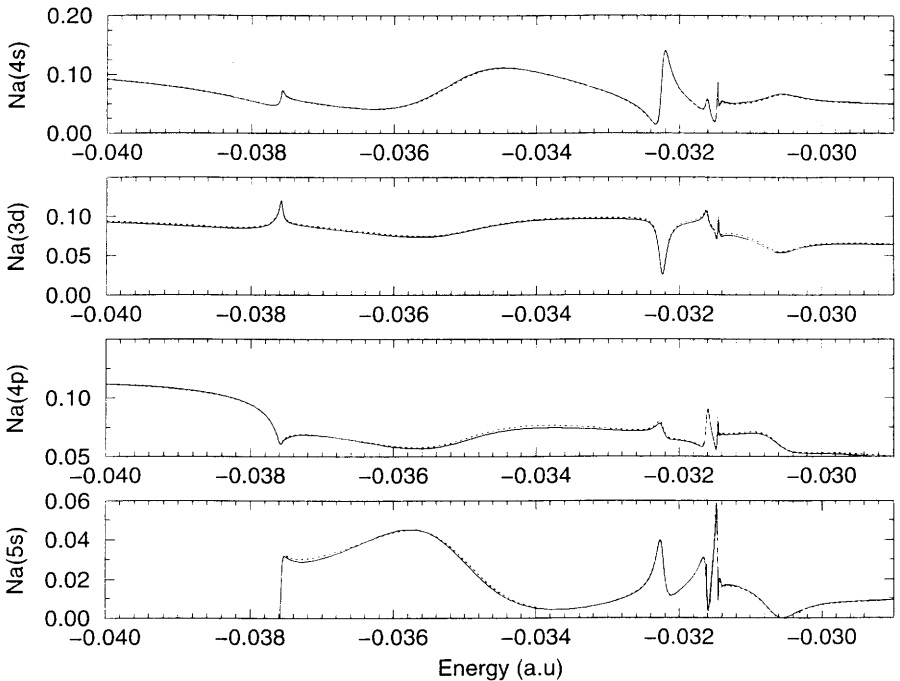


Figure 5: Eigenchannel R -matrix results¹⁸ for the process $\text{Na}^- + \gamma \rightarrow \text{Na}(nl) + e^-$ for $nl = 4s, 3d, 4p,$ and $5s$ plotted vs. energy (a.u.) below the double ionization threshold.

4 Na^- Photodetachment Partial Cross Sections

Comparison of Na^- with Li^- photodetachment is of interest because the core effect should play a larger role in Na^- than in Li^- . Once again, doubly excited states are responsible for the rich structure observed, which is more complex than found in H^- . Fig. 5 shows some partial cross sections.¹⁸ An interesting observation is that the detachment probability “sloshes” back and forth between the various partial cross sections as the energy increases. Thus, near an energy of -0.036 a.u. there are minima in the $\text{Li}(4s)$ and $\text{Li}(4p)$ partial cross sections but there is a maximum in the $\text{Li}(5s)$ partial cross section. At an energy of about -0.03 a.u., however, the minima have become local maxima and the maximum in $\text{Li}(5s)$ has become a minimum. One observes this behavior even on a very fine energy scale, such as, e.g., near $E = -0.0323$ a.u., where once again the $\text{Li}(5s)$ partial cross section has a local (resonance) maximum while this time the $\text{Li}(4s)$ and $\text{Li}(3d)$ partial cross sections have local (window resonance) minima. A more detailed discussion of our Na^- results, including comparisons with Li^- , is in preparation.¹⁸

5 Al^- Photodetachment Below the $\text{Al}(3s^2 4s^2 S)$ Threshold

We have carried out eigenchannel R -matrix calculations for $\text{Al}^-(3s^2 3p^2 \ ^3P)$ photodetachment from threshold to the $\text{Al}(3s^2 4s^2 S)$ threshold.¹⁹ In contrast to the negative alkali metal ions, Al^- as an unfilled p-subshell. In our calculations we treated the two outermost electrons as moving in an effective potential describing the $\text{Al}^+(3s^2 \ ^1S)$ core. An overview of our results is shown in Fig. 6. At the threshold one sees that the $\ ^3D^o$ and $\ ^3P^o$ partial cross sections behave as one expects, i.e., according to the Wigner threshold law. The inset shows excellent agreement with the relative measurements of Calabrese *et al.*²⁴ except at the highest energies. A striking feature, however, is the huge, narrow resonance just below the $\text{Al}(3s^2 4s^2 S)$ threshold. The experimental group of D. J. Larson has measured the detachment cross section just below this threshold. Fig. 7 shows that there is excellent agreement of theory and experiment on the position of this resonance. However, the theoretical prediction is narrower, which is what one expects given our approximation that we treat only two active electrons, thereby neglecting channels involving subvalence shells. Our calculations characterize this resonance as having predominantly $4s4p(\ ^3P^o)$ (56%) and $4s5p(\ ^3P^o)$ (30%) character. It is shown in Ref. 19 to have “+” character, with a large antinode on the Wannier ridge line, $r_1 = r_2$.

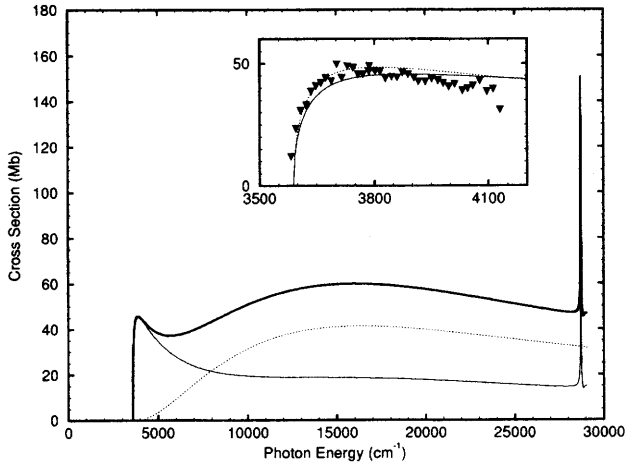


Figure 6: Calculated photodetachment cross section for Al^- from threshold and just above the first excited Al threshold using an eigenchannel R -matrix approach and the dipole length approximation. Thick solid curve: total cross section. Dotted curve: ${}^3D^0$ partial cross section. Thin solid curve: ${}^3P^0$ partial cross section. The inset shows dipole length (solid curve) and velocity (dotted curve) theoretical results in comparison with the relative measurements of Calabrese *et al.* (From Ref. 19.)

6 Conclusions

Our detailed studies of doubly excited state structures in photodetachment plus excitation of H^- , Li^- , Na^- , and Al^- allow some conclusions. First, this is a challenging area for both theory and experiment as obtaining the necessary predictions or measurements requires pushing current capabilities to their limits. Also, such joint theoretical and experimental efforts enable both to progress as each provides a valuable check for the other. Second, propensity rules applicable to pure three-body Coulomb systems seem to apply also to negative alkali and other negative ion spectra in that the “+” type resonances without angular nodal lines appear to dominate the observed and calculated spectra. Third, doubly-excited states that are quasi-forbidden in H^- photodetachment, become evident in negative alkali photodetachment spectra owing to the non-Coulomb core of the latter systems. Finally we note that among interesting areas for future work are (a) inclusion of sub-valence shells in theoretical studies of negative ions having open p-subshells, and (b) treatment of multiphoton detachment cross sections, as these may populate doubly excited states having different symmetries than those observed so far.

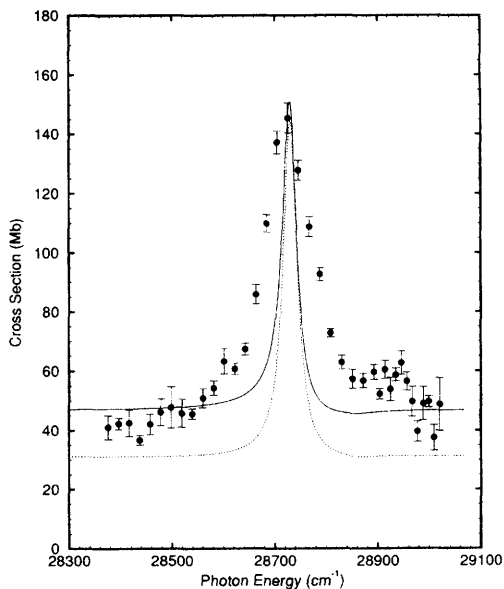


Figure 7: Calculated total photodetachment cross sections for Al^- in the photon energy region just below the first excited state threshold. Both dipole length (solid curve) and velocity (dashed curve) results are shown. Relative experimental data have been fit to the dipole length theoretical results using two parameters: the magnitude of the background cross section and the scaling factor to put the data on an absolute basis. (From Ref. 19.)

Acknowledgments

This work was supported in part by the U.S. Department of Energy, Office of Basic Energy Sciences, Division of Chemical Sciences under Grant No. DE-FG03-96ER14646.

References

1. R.P. Madden and K. Codling, *Phys. Rev. Lett.* **10**, 516 (1963).
2. J.W. Cooper, U. Fano and F. Pratts, *Phys. Rev. Lett.* **10**, 518 (1963).
3. J.H. Macek, *J. Phys. B* **1**, 831 (1968).
4. P.G. Harris, H.C. Bryant, A.H. Mohagheghi, R.A. Reeder, H. Sharifian, C.Y. Tang, H. Tootoonchi, J.B. Donahue, C.R. Quick, D.C. Rislove, W.W. Smith and J.E. Stewart, *Phys. Rev. Lett.* **65**, 309 (1990).

5. M. Domke, C. Xue, A. Puschmann, T. Mandel, E. Hudson, D.A. Shirley, G. Kaindl, C.H. Greene, H.R. Sadeghpour and H. Petersen, *Phys. Rev. Lett.* **66**, 1306 (1991).
6. H.R. Sadeghpour and C.H. Greene *Phys. Rev. Lett.* **65**, 313 (1990).
7. J.M. Röst and J.S. Briggs, *J. Phys. B* **23**, L339 (1990).
8. J.M. Röst, J.S. Briggs and J.M. Feagin, *Phys. Rev. Lett.* **66**, 1642 (1991).
9. H.R. Sadeghpour, *Phys. Rev. A* **43**, 5821 (1991).
10. H.R. Sadeghpour, C.H. Greene and M. Cavagnero, *Phys. Rev. A* **45**, 1587 (1992).
11. H.R. Sadeghpour and M. Cavagnero *J. Phys B* **26**, L271 (1993).
12. U. Fano and C.M. Lee, *Phys. Rev. Lett.* **31**, 1573 (1973).
13. P.F. O'Mahony and C.H. Greene, *Phys. Rev. Lett.* **31**, 250 (1985).
14. C.H. Greene and L. Kim, *Phys. Rev. A* **36**, 2706 (1987).
15. C.H. Greene in *Fundamental Processes of Atomic Dynamics* ed. J.S. Briggs, H. Kleinpoppen, and H.O. Lutz (Plenum, NY, 1988), p. 105.
16. C. Pan, A.F. Starace and C.H. Greene, *J. Phys. B* **27**, L137 (1994).
17. C. Pan, A.F. Starace and C.H. Greene, *Phys. Rev. A* **53**, 840 (1996).
18. C.N. Liu and A.F. Starace, *Phys. Rev. A* (to be published).
19. B.J. Davies, C.W. Ingram, D.J. Larson, C.N. Liu and A.F. Starace, *Phys. Rev. A* **56**, 378 (1997).
20. U. Berzinsh, G. Haefliger, D. Hanstorp, A. Klinkmüller, E. Lindroth, U. Ljungblad and D.J. Pegg, *Phys. Rev. Lett.* **74**, 4795 (1995).
21. E. Lindroth, *Phys. Rev. A* **53**, 2737 (1995).
22. C.D. Lin, *J. Phys B* **16**, 723 (1983).
23. U. Ljungblad, D. Hanstorp, U. Berzinsh, and D.J. Pegg, *Phys. Rev. Lett.* **77**, 3751 (1996).
24. D. Calabrese, A.M. Covington, J.S. Thompson, R.W. Marawar, and J.W. Farley, *Phys. Rev. A* **54**, 2797 (1996).